Original Article

High-resolution magnetic resonance imaging investigation of the connection between the triglyceride-glucose index and intracranial arterial remodeling: a retrospective cross-sectional study

Ya-Nan Niu[1,2#], Cong Guo[1,2#], Xuan-Zhu Guo[1,2], Qiao Wei[1,2], Xuan Zhou[1,2], Meng Li[1,2], Jia-Ning Xia[1,2], Li-Ping Chen[1,2]

[1]Department of Neurology, The Second Hospital of Hebei Medical University, Shijiazhuang, China; [2]Key Laboratory of Hebei Neurology, The Second Hospital of Hebei Medical University, Shijiazhuang, China

Contributions: (I) Conception and design: YN Niu, C Guo; (II) Administrative support: LP Chen; (III) Provision of study materials or patients: YN Niu, C Guo, XZ Guo, Q Wei, X Zhou, M Li, JN Xia; (IV) Collection and assembly of data: C Guo, YN Niu, XZ Guo, M Li, JN Xia; (V) Data analysis and interpretation: C Guo, YN Niu, Q Wei, X Zhou; (VI) Manuscript writing: All authors; (VII) Final approval of manuscript: All authors.

[#]These authors contributed equally to this work.

Correspondence to: Li-Ping Chen, PhD. Department of Neurology, The Second Hospital of Hebei Medical University, No. 215 Heping Road, Xinhua District, Shijiazhuang 050000, China; Key Laboratory of Hebei Neurology, The Second Hospital of Hebei Medical University, Shijiazhuang, China. Email: chenliping1950@126.com.

Background: Insulin resistance (IR) is associated with atherosclerotic plaque progression and the occurrence of stroke, with the triglyceride-glucose (TyG) index serving as a surrogate indicator. The present study aimed to investigate the association between TyG index levels and intracranial arterial remodeling in patients with acute ischemic stroke (AIS).

Methods: Patients with AIS who visited the Neurology Department of the Second Hospital of Hebei Medical University and underwent high-resolution magnetic resonance imaging (HR-MRI) between September 2018 and October 2021 were enrolled. A total of 123 patients were finally included in the study, with 81 excluded. The TyG index levels were measured, and the characteristics of intracranial atherosclerotic stenosis (ICAS) plaques were evaluated using HR-MRI. A logistic regression model was employed to analyze the relationship between TyG index levels and remodeling mode. Patients were divided into two groups, positive remodeling (PR) and non-positive remodeling (non-PR), based on the remodeling index (RI).

Results: Patients in the PR group had a higher TyG index than those in the non-PR group {median [interquartile range (IQR)]: 9.11 (8.82–9.51) *vs.* 8.72 (8.30–9.23), P<0.001}. After adjusting factors such as age and gender, the TyG index was found to be significantly correlated with intracranial arterial PR [odds ratio (OR): 3.169, 95% confidence interval (CI): 1.327–7.569, P=0.009]. In non-diabetes mellitus (DM) patients, the TyG index level in the PR group was significantly higher than that in the non-PR group (8.95±0.42 *vs.* 8.50±0.45, P<0.001), whereas there was no such difference in patients with DM.

Conclusions: TyG index was correlated with intracranial vessel PR, indicating that the TyG index level may be a useful marker for predicting intracranial vessel PR.

Keywords: Acute ischemic stroke (AIS); diabetes mellitus (DM); insulin resistance (IR); positive remodeling (PR); triglyceride-glucose index (TyG index)

Submitted May 26, 2023. Accepted for publication Sep 25, 2023. Published online Nov 06, 2023.
doi: 10.21037/qims-23-752
View this article at: https://dx.doi.org/10.21037/qims-23-752

Introduction

Intracranial atherosclerotic stenosis (ICAS) is the leading cause of stroke and the second leading cause of death worldwide with a high incidence of morbidity and mortality (1,2). The narrowing of the arterial lumen due to the formation of atherosclerotic plaques prompts structural modifications in blood vessels, referred to as vascular remodeling. It is an adaptive change in blood vessels that involves modifications to the intima, tunica media, and tunica adventitia and is associated with apoptosis, hyperplasia, and rearrangement of vascular endothelial cells, macrophages, and other cells (3). Previous research has demonstrated that positive remodeling (PR) of the carotid artery causes acute ischemic stroke (AIS) and is associated with the characteristics of vulnerable plaques (4).

Insulin resistance (IR) is a systemic pathological condition in which insulin responses are less than the expected biological effect. According to studies, IR can promote the progression and increased instability of atherosclerotic plaques by inducing platelet activation, endothelial dysfunction, and a chronic systemic inflammatory state, thereby increasing the risk of stroke (5). With high accuracy and specificity in identifying IR using hyper insulinemic-euglycemic clamp (HIEC) and homeostasis model assessment of IR (HOMA-IR) as reference standards, the triglyceride-glucose index (TyG index) is regarded as a simple and reliable surrogate indicator for IR (6,7). TyG index, which is an all-encompassing reflection of blood glucose and the triglycerides (TG) level, is calculated using the formula Ln [fasting TG (mg/dL) × fasting blood glucose (FBG; mg/dL)/2]. According to previous studies, TyG index is associated with nonalcoholic fatty liver disease (NAFLD) (8,9), carotid atherosclerosis (10), instable plaques of the carotid artery (11), arterial stiffness (12), a high risk of coronary arterial calcification (13), and poor prognosis of stroke. However, there have been few studies on the relationship between the TyG index level and intracranial vascular remodeling and vulnerable plaque characteristics.

In this study, we aimed to examine the relationship between the IR of the TyG index and intracranial vascular remodeling and ICAS plaque features in AIS patients using high-resolution magnetic resonance imaging (HR-MRI), which permits quantitative and qualitative analyses of plaque characteristics (14). We present this article in accordance with the STROBE reporting checklist (available at https://qims.amegroups.com/article/view/10.21037/qims-23-752/rc).

Methods

Participants

This is a retrospective cross-sectional study. Patients with AIS who visited the Neurology Department of the Second Hospital of Hebei Medical University and underwent HR-MRI imaging between September 2018 and October 2021 were enrolled.

The inclusion criteria were as follows: (I) patients with AIS diagnosed within 2 weeks of onset by computed tomography (CT) or diffusion-weighted imaging (DWI); (II) patients examined by HR-MRI imaging within 2 weeks of onset of symptoms; (III) patients with at least one atherosclerotic plaque identified in the offending vessel area by HR-MRI imaging.

The exclusion criteria were as follows: (I) extracranial carotid artery or vertebral artery stenosis ≥30% on the same side as a cerebral infarction or obvious vulnerable plaque features; (II) patients with intracranial arterial lesions such as vasculitis, cerebrovascular malformation, fibromuscular dysplasia, dissection, or moyamoya disease who had experienced a stroke; (III) patients with cardiac embolism risk factors including atrial fibrillation and atrial/ventricular septal defect; (IV) patients with severe respiratory, circulatory, or renal failure; (V) patients with acute infection, malignancy, or other conditions; (VI) patients with missing clinical data; (VII) patients with poor image quality.

This study was conducted in accordance with the Declaration of Helsinki (as revised in 2013) and approved by the Ethics Committee of The Second Hospital of Hebei Medical University. Written informed consent was provided by all participants.

Clinical data and laboratory measurement

Baseline data of registered patients: the medical history

of gender, age, height, weight, smoking, drinking, and hypertension (systolic pressure ≥140 mmHg and/or diastolic pressure ≥90 mmHg, or taking hypotensive drugs currently), the medical history of diabetes mellitus (DM) [FBG ≥7.0 mmol/L, random glucose ≥11.1 mmol/L, or glycated hemoglobin (HbA1c) ≥7%, or taking hypoglycemic drugs currently], dyslipidemia [total cholesterol (TC) ≥5.18 mmol/L, TG ≥1.7 mmol/L, low-density lipoprotein (LDL) ≥3.37 mmol/L, high-density lipoprotein (HDL) <1.04 mmol/L]. The National Institutes of Health Stroke Score (NIHSS) of patients was evaluated after admission, with a score of ≤4 points defined as no or minor stroke, and a score >5 defined as moderate and more severe stroke.

Venous blood test results were collected the day after admission and fasting overnight, including the levels of white blood cells (WBC), homocysteine (Hcy), LDL, HDL, TC, TG, high-sensitivity C-reactive protein (hs-CRP), FBG, HbA1c, apolipoprotein A1 (apoA1), and apolipoprotein B (apoB).

TyG index was calculated using the formula TyG = Ln [fasting TG (mg/dL) × FBG (mg/dL)/2], and body mass index (BMI) was calculated using the formula BMI = weight (kg)/height^2 (m^2).

MRI scheme

All patients were imaged with a 3.0 T MRI scanner (Philips Healthcare, Best, Netherlands) equipped with an 8-channel phased array head coil and a 16-channel neurovascular coil. T1-weighted imaging (T1WI), T2-weighted imaging (T2WI), T2-weighted fluid-attenuated inversion recovery (T2-FLAIR), DWI, and apparent diffusion coefficient (ADC) sequences comprised the standard protocol for whole-brain imaging. Images of the vessel wall were acquired using T1-weighted sequences (volume isotropic turbine spin echo acquisition) before and after contrast agent injection: (I) repetition time (TR) =800/900 ms, echo time (TE) =18/24 ms, field of view (FOV) =200×181×45/158×158×158 mm^3, matrix =332×300×150/256×256×246, layer thickness: 0.6 mm, acquisition time =7 min 1 s/8 min 6 s. Vessel wall enhanced imaging was performed 5 minutes after intravenous injection of gadopentetate meglumine (dosage: 0.1 mmol/kg). (II) The imaging parameters of three-dimensional (3D) time of flight (TOF) magnetic resonance angiography (MRA) are as follows: TR =25/21 ms, TE =3.5/3.6 ms, FOV =180×180/173×199 mm^2, matrix =300×300/384×301, layer thickness: 0.6 mm, acquisition time =5 min 39 s/6 min.

Image analysis

The HR-MRI images of all patients were independently analyzed by two neuroradiologists with more than 3 years of experience and no knowledge of the clinical information and research content using the VesselMass software (Leiden University Medical Center, Leiden, Netherlands). In cases where interpretation results differed, another senior neuroradiologist (with more than 10 years of experience) re-evaluated the images and assisted the two neuroradiologists in coming to an agreement.

Using the multi-plane reconstruction tool in the VesselMass software, the long and short axes of the blood vessels at the site of maximum stenosis on the T1-weighted image were reconstructed. The lumen wall was manually delineated at its narrowest point on the obtained cross-sectional image. The reference region was defined as the proximal and distal ends of the maximum stenosis segment or the plaque-free region (with the average area calculated) (15). The atherosclerotic plaque was defined as eccentric wall thickening with or without lumen stenosis on the vessel wall image after reconstruction of the pre-enhanced and/or post-enhanced T1-weighted volume isotropic turbo spin-echo acquisition (T1-VISTA) image; the offending plaque was defined as the only or narrowest lesion in the vascular region of ischemic stroke (16,17). Vulnerable plaque features included plaque enhancement, intra-plaque hemorrhage, plaque surface irregularities, and remodeling patterns.

The following data were automatically output by the software: lumen diameter (LD), maximum wall thickness (MaxWT), total vascular area (TVA), and lumen area (LA). Wall area (WA) = TVA – LA. The plaque length was measured on the long axis of the plaque. In calculation, stenosis =1 – $LD_{stenosis}/LD_{reference}$; normalized wall index (NWI) = $WA_{stenosis}/TVA_{stenosis}$ (18), representing the plaque load; on the post-enhanced image, the plaque with the enforcement similar to or higher than that of the pituitary stalk was defined as being strongly enhanced (19); the plaque in which the signal intensity was greater than 150% of that of the adjacent muscle on the pre-enhanced T1-VISTA image was considered T1 high signal, which could determine intraplaque hemorrhage (20-22); irregular surface referred to the discontinuity of the plaque surface. Remodeling index (RI) was calculated by RI = $TVA_{stenosis}/TVA_{reference}$, of which RI ≥1.05 represents PR (*Figure 1*), and RI <1.05 represents non-positive remodeling (non-PR).

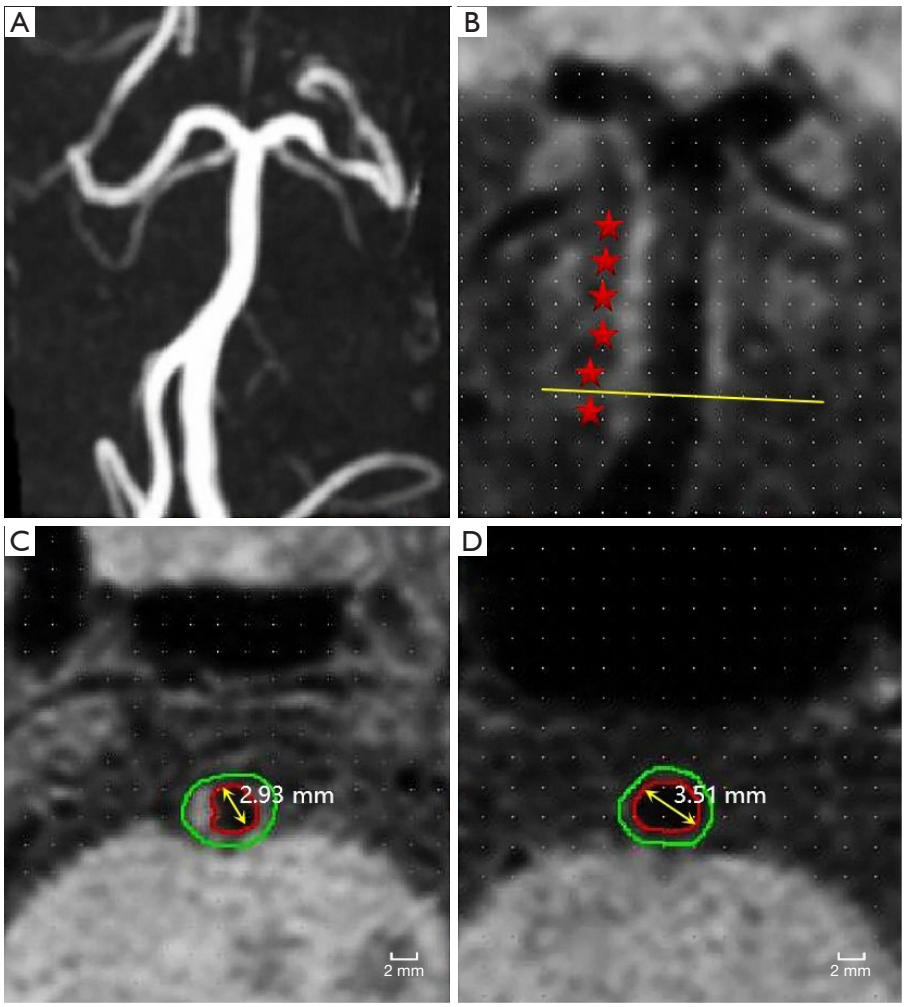

Figure 1 Basilar arterial PR of a patient with acute ischemic stroke. (A) MRA image of the vertebrobasilar artery of the patient. (B) Pre-enhanced 3D T1-VISTA of the basilar arterial wall reveals atherosclerotic plaque (red asterisks). The maximum narrow plane is marked by the yellow line. (C,D) A short-axis image was reconstructed perpendicular to the basilar artery, and the lumen (red) and tube wall (green) of the narrowest section (C) and the reference section (D) were manually drawn on the cross-sectional image. Calculation of vascular RI: output the data of TVA using the software automatically. RI was calculated by RI = $TVA_{stenosis}/TVA_{reference}$, with PR defined as RI ≥1.05 and non-PR defined as RI <1.05, RI =0.1844/0.1620 =1.14 >1.05, indicating that this blood vessel is PR. MRA, magnetic resonance angiography; 3D, three-dimensional; T1-VISTA, T1-weighted volume isotropic turbo spin-echo acquisition; RI, remodeling index; TVA, total vascular area; PR, positive remodeling.

Statistical analysis

Continuous variables were summarized by mean ± standard deviation (SD) or median [interquartile range (IQR)], whereas classified variables were summarized as counts and percentages. Continuous variables were statistically analyzed by independent sample *t*-test or non-parametric Mann-Whitney *U* test, and classified variables were statistically analyzed by the Chi-squared test. A multivariate logistic regression model was constructed to evaluate the correlation between the TyG index level and the offending vessel PR, and the odds ratio (OR) and 95% confidence interval (CI) were calculated. Subgroup analysis was performed to discuss the relationship between the TyG index and the vessel PR in DM and non-diabetic (non-DM) patients. Plaque load and RI measurements were subjected to an intraclass correlation coefficient (ICC) analysis to ensure that there was interobserver and intraobserver

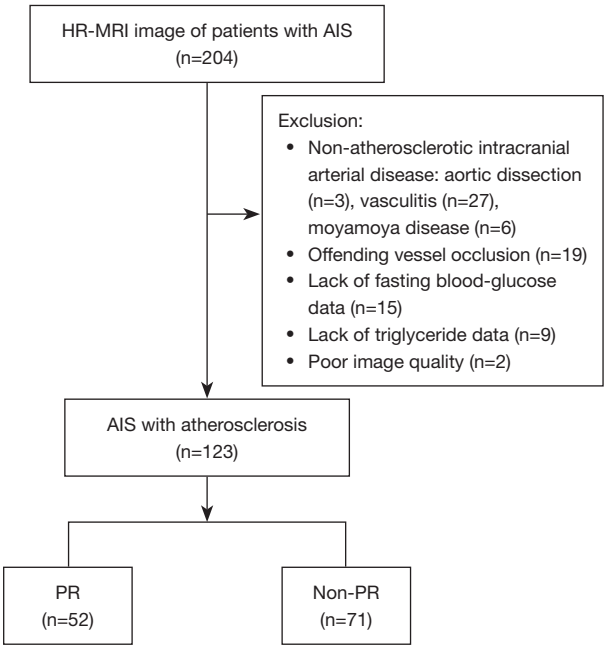

Figure 2 Flowchart of screening of included patients. HR-MRI, high-resolution magnetic resonance imaging; AIS, acute ischemic stroke; PR, positive remodeling.

agreement. All statistical analyses were performed using SPSS 26.0 (IBM Corp., Armonk, NY, USA). A P value <0.05 indicated a statistically significant difference.

Results

HR-MRI images of 204 patients from September 2018 to October 2021 were collected; 123 patients were finally included in the study, with 81 excluded for the following reasons: 36 with non-atherosclerotic intracranial arterial disease [including aortic dissection (n=3), vasculitis (n=27), moyamoya disease (n=6)], offending vessel occlusion (n=19), lack of FBG (n=15) or TG (n=9) data, and poor image quality (n=2). The screening process of included patients is shown in *Figure 2*.

Comparison of clinical and imaging data of patients

A total of 123 patients were included in the study, with the mean age of 53.8±12.4 years; 81 (65.9%) cases were male; 83 (67.5%) had hypertension; 49 (39.8%) had DM; 90 (73.2%) had dyslipidemia; and 52 (42.3%) had offending vessel PR. The median TyG index was 8.96 (8.50–9.39). *Table 1* displays the results of a comparison between clinical and imaging data pertaining to the underlying vascular remodeling mode in AIS patients.

Patients with PR had higher levels of Hcy, TC, TG, LDL, apoB, FBG, and TyG index than those with non-PR. In the latter, the likelihood of moderate and above degree stroke was higher [25 (48.1%) *vs.* 17 (23.9%), P=0.005], the degree of vessel stenosis was lower (40.5%±18.5% *vs.* 48.7%±17.7%, P=0.015), whereas the WA [0.15 (0.13–0.21) *vs.* 0.11 (0.09–0.16) mm^2, P<0.001], MaxWT [2.37 (1.92–2.76) *vs.* 1.77 (1.42–2.16) mm, P<0.001] and plaque length [7.77 (6.52–9.32) *vs.* 6.80 (4.95–8.09) mm, P=0.003] were higher. Other characteristics were also examined and found to be identical in both groups.

Logistic regression analysis of PR and vascular risk factors

Although Hcy, apoB, and TyG index were all significantly correlated with PR in univariate analyses, only the TyG index remained significantly correlated with intracranial arterial PR in multivariate analyses after adjusting for age, gender, smoking, drinking, hypertension, DM, dyslipidemia, Hcy, TC, LDL, and apoB (OR: 3.169, 95% CI: 1.327–7.569, P=0.009) (*Table 2*).

Subgroup analysis of DM and non-DM patients

Patients were categorized as having DM (n=49) or not having DM (n=74) based on the presence of DM. Among the DM patients, 22 had PR in the offending vessel whereas 27 were non-PR. Patients in the PR group were more likely to be female, and have higher TC, LDL, and apoB levels, less degree of stenosis, and larger MaxWT and WA (P<0.05) compared to the non-PR group. Other characteristics did not differ between the two groups. There were 30 patients with PR in the offending vessel and 44 patients without PR in the offending vessel in the non-DM group. Higher levels of Hcy, TG, FBG, HbA1c, apoB, and TyG indices, as well as longer plaques, and larger MaxWT and WA, and the higher moderate-severe stroke were found in the PR group compared to the non-PR group at P<0.05. No differences were found in other features between the two groups (*Table 3*).

Logistic regression analysis of PR and vascular risk factors in non-DM patients

Univariate logistic regression showed that the TyG index was related to intracranial arterial PR (OR: 2.952, 95% CI: 1.619–5.383, P<0.001), and multivariate logistic regression,

Table 1 Comparison of clinical and imaging data between PR and non-PR patients

Item	Total patients (n=123)	Non-PR (n=71)	PR (n=52)	P value
Clinical features				
Age (years)	53.8±12.4	54.5±13.5	52.9±11.0	0.467
Male	81 (65.9)	47 (66.2)	34 (65.4)	0.925
BMI (kg/m^2)	24.2 (22.9–26.6)	23.9 (22.8–26.6)	24.8 (23.2–27.3)	0.324
Smoking	42 (34.1)	22 (31.0)	20 (38.5)	0.388
Drinking	28 (22.8)	15 (21.1)	13 (25.0)	0.613
Hypertension	83 (67.5)	47 (66.2)	36 (69.2)	0.723
DM	49 (39.8)	27 (38.0)	22 (42.3)	0.632
Dyslipidemia	90 (73.2)	48 (67.6)	42 (80.8)	0.104
Moderate-severe stroke	42 (34.1)	17 (23.9)	25 (48.1)	0.005
Biochemical indicators				
WBC (×10^9/L)	6.24 (5.34–7.33)	6.24 (5.34–7.33)	6.25 (5.32–7.59)	0.808
hs-CRP (mg/L)	1.80 (0.90–3.50)	1.90 (1.20–3.10)	1.58 (0.80–4.05)	0.570
Hcy (μmol/L)	13.1 (9.90–16.8)	12.4 (9.60–16.0)	14.9 (11.3–1.8.4)	0.025
TC (mmol/L)	4.02 (3.46–4.70)	3.80 (3.36–4.49)	4.39 (3.88–5.10)	0.009
TG (mmol/L)	1.59 (1.13–2.04)	1.41 (0.99–1.87)	1.76 (1.31–2.19)	0.005
HDL-C (mmol/L)	1.03 (0.89–1.24)	1.04 (0.89–1.26)	1.03 (0.89–1.23)	0.937
LDL-C (mmol/L)	2.47 (1.99–3.06)	2.25 (1.87–2.86)	2.76 (2.38–3.55)	0.003
apoA1 (g/L)	1.19 (0.99–2.10)	1.20 (0.99–6.00)	1.18 (0.99–1.76)	0.549
apoB (g/L)	0.82 (0.69–1.06)	0.74 (0.67–0.92)	0.96 (0.80–1.10)	<0.001
FBG (mmol/L)	5.72 (5.01–7.38)	5.29 (4.93–6.39)	6.34 (5.33–8.04)	0.001
HbA1c (%)	5.90 (5.50–7.50)	5.80 (5.30–7.10)	6.00 (5.60–7.95)	0.080
TyG index	8.96 (8.50–9.39)	8.72 (8.30–9.23)	9.11 (8.82–9.51)	<0.001
Imaging data				
Stenosis (%)	45.2±18.5	48.7±17.7	40.5±18.5	0.015
MaxWT (mm)	2.00 (1.57–2.53)	1.77 (1.42–2.16)	2.37 (1.92–2.76)	<0.001
WA (mm^2)	0.13 (0.10–0.18)	0.11 (0.09–0.16)	0.15 (0.13–0.21)	<0.001
Plaque length (mm)	7.32 (5.47–8.69)	6.80 (4.95–8.09)	7.77 (6.52–9.32)	0.003
NWI (%)	87.0 (79.0–92.0)	86.1 (77.0–91.0)	87.1 (79.0–93.0)	0.361
Strongly enhanced (plaque)	51 (41.5)	30 (42.3)	21 (40.4)	0.835
T1 high signal (plaque)	19 (15.4)	13 (18.3)	6 (11.5)	0.305
Irregular surface (plaque)	56 (45.5)	29 (40.8)	27 (51.9)	0.223

Continuous variables with a normal distribution were expressed as mean ± standard deviation, continuous variables with a non-normal distribution were expressed as median (interquartile range). Classified variables were summarized as counts (percentages). PR, positive remodeling; BMI, body mass index; DM, diabetes mellitus; WBC, white blood cell; hs-CRP, high-sensitivity C-reactive protein; Hcy, homocysteine; TC, total cholesterol; TG, triglyceride; HDL-C, high-density lipoprotein cholesterol; LDL-C, low-density lipoprotein cholesterol; apoA1, apolipoprotein A1; apoB, apolipoprotein B; FBG, fasting blood glucose; HbA1c, glycated hemoglobin; TyG, triglyceride-glucose; MaxWT, maximum wall thickness; WA, wall area; NWI, normalized wall index.

Table 2 Logistic regression analysis of PR and cardiovascular risk factors

Item	Univariate logistic regression		Multivariate logistic regression*	
	OR (95% CI)	P value	OR (95% CI)	P value
Age (years)	0.989 (0.961–1.018)	0.464	0.995 (0.961–1.030)	0.767
Gender	0.965 (0.454–2.050)	0.925	0.78 (0.315–2.452)	0.805
Smoking	1.392 (0.656–2.952)	0.388	1.001 (0.321–3.123)	0.999
Drinking	1.244 (0.533–2.905)	0.613	0.966 (0.286–3.260)	0.956
Hypertension	1.149 (0.533–2.474)	0.723	1.001 (0.407–2.462)	0.998
DM	1.195 (0.576–2.479)	0.632	0.526 (0.195–1.414)	0.203
Dyslipidemia	2.012 (0.860–4.709)	0.107	1.114 (0.425–2.921)	0.826
Hcy (mmol/L)	1.057 (1.001–1.115)	0.045	1.049 (0.988–1.115)	0.120
TC (mmol/L)	1.284 (0.964–1.711)	0.087	0.879 (0.371–2.068)	0.762
LDL-C (mmol/L)	1.317 (0.947–1.832)	0.101	0.988 (0.348–2.803)	0.982
apoB (g/L)	4.214 (1.224–14.510)	0.023	3.032 (0.087–104.462)	0.541
TyG index	2.766 (1.460–5.239)	0.002	3.169 (1.327–7.569)	0.009

*, adjusted for age, sex, hypertension, DM, smoking, drinking, Hcy, TC, apoB, and LDL-C. PR, positive remodeling; OR, odds ratio; CI, confidence interval; DM, diabetes mellitus; Hcy, homocysteine; TC, total cholesterol; LDL-C, low-density lipoprotein cholesterol; apoB, apolipoprotein B; TyG, triglyceride-glucose.

which included age, gender, smoking, drinking, hypertension, Hcy, TC, LDL-C, apoB, and the TyG index, showed that the TyG index were significantly correlated with PR (OR: 4.183, 95% CI: 1.749–10.008, P=0.001) (*Table 4*).

Linear regression analysis of TyG index and vascular risk factors

The linear regression analysis of the association between the TyG index and vascular risk factors revealed an association between the TyG index and hypertension, DM, BMI, WBC, TC, TG, LDL, apoB, FBG, and HbA1c (*Table 5*).

Reproducibility

Measurement consistency between observers in imaging data was investigated using the ICC. The measurement of plaque MaxWT (ICC: 0.909, 95% CI: 0.689–0.977, P<0.001), plaque length (ICC: 0.818, 95% CI: 0.453–0.951, P=0.001), NWI (ICC: 0.910, 95% CI: 0.494–0.987, P=0.003), and vessel RI (ICC: 0.952, 95% CI: 0.432–0.997, P=0.001) had good interobserver consistency.

Discussion

In this study, we looked at how the TyG index relates to the vascular remodeling pattern seen in patients with AIS. TyG index was significantly correlated with intracranial vessel PR after adjusting for age, gender, smoking, alcohol consumption, blood pressure, DM, dyslipidemia, HDL, LDL, and apoB in a multivariate logistic regression analysis. In the non-DM group, the TyG index was found to be independently correlated with vessel PR. In conclusion, our results indicate that the TyG index level may be a useful marker for predicting intracranial vessel PR, particularly in non-DM patients.

In healthy people, IR contributes to increased plasma TG and FBG levels, and hyperglycemia and hyperlipidemia can impair insulin activity and exacerbate IR. There is a vicious cycle formed by their interaction. HIEC, a golden standard for evaluating IR, has limited application in clinical settings due to its complexity, making the TyG index an appealing alternative strategy. As a simple and reliable surrogate indicator for IR, the TyG index has been the subject of numerous studies due to its high accuracy and specificity in identifying IR with HIEC as the reference standard (23-25).

When vessels undergo vascular remodeling, they are subjected to structural and functional changes as a result of an adaptive process. Intraplaque hemorrhage and ulceration, with inflammation and hyperplasia, have been linked to PR as the main pathological changes. Kim *et al.* discovered a strong association between IR and coronary arterial PR (26). As a proxy for IR, the TyG index

Table 3 Comparison of features between DM and non-DM patients

Item	Non-DM				DM			
	Total patients (n=74)	Non-PR (n=44)	PR (n=30)	P value	Total patients (n=49)	Non-PR (n=27)	PR (n=22)	P value
Clinical features								
Age (years)	52.5±13.4	53.3±14.5	51.3±11.9	0.532	55.7±10.6	56.4 ±11.6	54.9±9.5	0.627
Male	49 (66.2)	26 (59.1)	23 (76.7)	0.117	32 (65.3)	21 (77.8)	11 (50.0)	0.042
BMI (kg/m^2)	23.5 (22.5–26.2)	23.5 (22.2–25.7)	24.3 (23.0–26.9)	0.099	25.2 (23.7–27.7)	25.7 (23.9–27.7)	25.0 (23.2–27.4)	0.488
Smoking	25 (33.8)	13 (29.5)	12 (40.0)	0.351	17 (34.7)	9 (33.3)	8 (36.4)	0.825
Drinking	20 (27.0)	10 (22.7)	10 (33.3)	0.313	8 (16.3)	5 (18.5)	3 (13.6)	0.715
Hypertension	42 (56.8)	23 (52.3)	19 (63.3)	0.346	41 (83.7)	24 (88.9)	17 (77.3)	0.274
Dyslipidemia	33 (44.6)	15 (34.1)	18 (60.0)	0.483	31 (63.3)	17 (63.0)	14 (63.6)	0.961
Moderate-severe stroke	24 (32.4)	9 (20.5)	15 (50.0)	0.008	18 (36.7)	8 (29.6)	10 (45.5)	0.487
Biochemical indicators								
WBC (×10^9/L)	6.02 (5.23–7.26)	6.02 (5.21–7.37)	5.98 (5.26–7.10)	0.895	6.51 (5.63–7.78)	6.60 (5.60–7.24)	6.39 (5.60–8.40)	0.849
hs-CRP (mg/L)	1.65 (0.90–3.33)	1.65 (1.05–2.45)	1.95 (0.88–4.13)	0.593	2.10 (1.05–5.00)	2.60 (1.20–5.20)	1.48 (0.80–3.83)	0.114
Hcy (μmol/L)	13.2 (9.70–16.7)	12.5 (9.13–16.2)	14.7 (11.4–20.6)	0.050	13.0 (10.1–17.4)	12.2 (10.0–15.1)	16.2 (10.6–18.1)	0.265
TC (mmol/L)	3.94 (3.39–4.57)	3.75 (3.38–4.41)	4.34 (3.59–4.99)	0.159	4.30 (3.64–5.26)	3.99 (3.29–4.81)	4.50 (4.21–5.76)	0.014
TG (mmol/L)	1.29 (0.99–1.82)	1.11 (0.96–1.60)	1.74 (1.23–1.93)	0.002	1.75 (1.44–2.46)	1.41 (0.99–1.87)	1.98 (1.53–2.57)	0.644
HDL-C (mmol/L)	1.03 (0.90–1.28)	1.04 (0.95–1.32)	1.00 (0.88–1.18)	0.293	1.04 (0.89–1.23)	1.02 (0.88–1.20)	1.07 (0.94–1.25)	0.282
LDL-C (mmol/L)	2.42 (1.95–2.89)	2.29 (1.89–2.91)	2.59 (2.07–3.02)	0.266	2.54 (2.02–3.58)	2.16 (1.86–2.60)	2.99 (2.54–4.20)	0.002
apoA1 (g/L)	1.34 (1.06–9.63)	1.39 (1.05–14.0)	1.25 (1.10–7.03)	0.370	1.06 (0.91–1.29)	1.04 (0.87–1.25)	1.12 (0.93–1.31)	0.658
apoB (g/L)	0.80 (0.69–0.97)	0.73 (0.67–0.85)	0.89 (0.79–1.06)	0.017	0.88 (0.73–1.16)	0.77 (0.67–1.13)	1.03 (0.88–1.41)	0.004
FBG (mmol/L)	5.26 (4.90–5.84)	5.00 (4.74–5.33)	5.71 (5.26–6.47)	<0.001	7.83 (6.09–10.2)	7.10 (5.93–9.65)	8.01 (6.52–11.4)	0.112
HbA1c (%)	5.60 (5.30–5.80)	5.50 (5.23–5.80)	5.75 (5.40–5.90)	0.038	7.90 (6.75–9.30)	7.70 (6.50–9.10)	8.20 (7.13–9.53)	0.195
TyG index	8.68±0.49	8.50±0.45	8.95±0.42	<0.001	9.39±0.65	9.28±0.56	9.52±0.73	0.201
Imaging data								
Stenosis (%)	43.4±18.5	45.6±17.4	40.1±20.0	0.218	48.0±18.2	53.7±17.4	41.0±16.9	0.013
MaxWT (mm)	1.91 (1.49–2.37)	1.72 (1.37–2.09)	2.27 (1.81–2.62)	0.001	2.16 (1.60–2.77)	1.80 (1.44–2.74)	2.55 (2.12–2.93)	0.005
WA (mm^2)	0.12 (0.10–0.18)	0.10 (0.09–0.15)	0.15 (0.12–0.22)	<0.001	0.16 (0.11–0.20)	0.13 (0.08–0.16)	0.17 (0.15–0.21)	0.018
Plaque length (mm)	7.29 (5.20–8.60)	6.11 (4.63–7.77)	8.07 (6.84–10.9)	0.001	7.40 (5.81–9.17)	7.05 (5.42–9.23)	7.49 (6.16–9.16)	0.755
NWI (%)	85.0 (77.0–92.0)	83.2 (77.0–89.7)	86.9 (77.8–93.0)	0.273	89.0 (81.1–92.5)	89.0 (81.4–92.0)	87.1 (80.3–93.3)	0.880
Strongly enhanced (plaque)	33 (44.6)	18 (40.9)	15 (50.0)	0.440	18 (36.7)	12 (44.4)	6 (27.3)	0.215
T1 high signal (plaque)	12 (16.2)	9 (20.5)	3 (10.0)	0.339	7 (14.3)	4 (14.8)	3 (13.6)	1.000
Irregular surface (plaque)	41 (55.4)	28 (63.6)	13 (43.3)	0.085	26 (53.1)	14 (51.9)	12 (54.5)	0.851

Continuous variables with a normal distribution were expressed as mean ± SD (standard deviation), continuous variables with a non-normal distribution were expressed as median (interquartile range). Classified variables were summarized as counts (percentages). DM, diabetes mellitus; PR, positive remodeling; BMI, body mass index; WBC, white blood cell; hs-CRP, high-sensitivity C-reactive protein; Hcy, homocysteine; TC, total cholesterol; TG, triglyceride; HDL-C, high-density lipoprotein cholesterol; LDL-C, low-density lipoprotein cholesterol; apoA1, apolipoprotein A1; apoB, apolipoprotein B; FBG, fasting blood glucose; HbA1c, glycated hemoglobin; TyG, triglyceride-glucose; MaxWT, maximum wall thickness; WA, wall area; NWI, normalized wall index.

Table 4 Logistic regression analysis of PR and vascular risk factors

Item	Univariate logistic regression		Multivariate logistic regression*	
	OR (95% CI)	P value	OR (95% CI)	P value
Age (years)	0.989 (0.955–1.024)	0.527	0.970 (0.921–1.021)	0.242
Gender	2.275 (0.806–6.421)	0.121	4.128 (0.836–20.394)	0.082
Smoking	1.590 (0.599–4.220)	0.352	1.045 (0.151–7.250)	0.965
Drinking	1.700 (0.603–4.791)	0.315	0.202 (0.020–2.005)	0.172
Hypertension	1.577 (0.610–4.075)	0.347	2.332 (0.598–9.097)	0.223
Hcy (mmol/L)	1.072 (0.997–1.152)	0.059	1.110 (1.000–1.232)	0.049
TC (mmol/L)	1.083 (0.747–1.570)	0.673	3.677 (0.891–15.175)	0.072
LDL-C (mmol/L)	0.993 (0.646–1.528)	0.975	0.025 (0.180–1.324)	0.092
apoB (g/L)	1.911 (0.394–10.075)	0.405	1.231 (0.169–8.949)	0.837
TyG index	2.952 (1.619–5.383)	<0.001	4.183 (1.749–10.008)	0.001

*, adjusted for age, sex, hypertension, smoking, drinking, Hcy, TC, apoB and LDL-C. PR, positive remodeling; OR, odds ratio; CI, confidence interval; Hcy, homocysteine; TC, total cholesterol; LDL-C, low-density lipoprotein cholesterol; apoB, apolipoprotein B; TyG, triglyceride-glucose.

Table 5 Linear regression analysis of TyG index and vascular risk factors

Item	TyG index	
	r	P value
Clinical features		
Hypertension	0.197	0.029
DM	0.529	0.000
BMI (kg/m^2)	0.206	0.022
Biochemical indicators		
WBC (×10^9/L)	0.241	0.007
TC (mmol/L)	0.278	0.002
TG (mmol/L)	0.860	0.000
LDL-C (mmol/L)	0.193	0.032
apoB (g/L)	0.354	0.000
FBG (mmol/L)	0.755	0.000
HbA1c (%)	0.692	0.000

TyG, triglyceride-glucose; DM, diabetes mellitus; BMI, body mass index; WBC, white blood cell; TC, total cholesterol; TG, triglyceride; LDL-C, low-density lipoprotein cholesterol; apoB, apolipoprotein B; FBG, fasting blood glucose; HbA1c, glycated hemoglobin.

reflects both glucose toxicity and lipid toxicity. Increased blood glucose, lipids, and insulin trigger endothelial cell inflammation, which in turn recruits leukocytes to degrade extracellular matrix via matrix metalloproteinase secretion; vascular remodeling is induced, resulting in vasodilation; and cytokines and extracellular matrix protein are secreted to aid in the process (27-29). Platelet activation, adhesion, and aggregation are promoted by leukocyte interaction with the adhesion protein expressed on the endothelial barrier of inflammation, which in turn promotes the progression of atherosclerosis. Interaction between pro-inflammatory factors and platelets further promotes the pro-inflammatory and pro-thrombosis functions of platelets and endothelial cells, which is involved in vascular remodeling.

Changes in local hemodynamics also contribute to the development of new blood vessel structures (30). High wall shearing stress stimulation has been found to cause vessel PR in many cases. Plaque formation causes lumen stenosis, which boosts local blood flow velocity and activates endothelial inflammation, both of which contribute to PR. Furthermore, elevated insulin under the IR state causes vasoconstriction and reabsorption of water and sodium in the renal tubule by stimulating increased sympathetic nerve discharge, angiotensin II, aldosterone, and endothelin

synthesis; extracellular hyperosmosis due to hyperglycemia causes an increase in the circulating blood volume, resulting in an increase in blood pressure (31,32). Inflammatory mechanisms contribute to vascular remodeling, and the increased wall pressure alters the phenotype of vascular smooth muscle (33).

The results of our study also revealed that PR was significantly correlated with apoB and Hcy levels, and that patients in the PR group had significantly higher apoB and Hcy levels compared to patients in the non-PR group. Although an increase in TG is the defining feature of atherosclerotic dyslipidemia, it is not the direct substance causing atherosclerosis; rather, the imbalance between TG-rich apoB and apoA1 (such as HDL) is the primary cause of atherosclerotic dyslipidemia (34,35). ApoB is considered an indicator of oxidation and atherosclerotic features. According to research by Wang *et al.*, apoB may be a ligand that stimulates MMP-9 expression and secretion, which in turn promotes vessel PR (36). It has been shown in the past that hyperhomocysteinemia is an independent risk factor for cardiovascular and cerebrovascular diseases, and that it may contribute to the development of atherosclerosis and vascular remodeling by promoting the proliferation and migration of vascular smooth muscle cells, activating the inflammatory response, and increasing oxidative stress (37). Similarly, Lu *et al.* found that elevated Hcy levels were associated with decreased PR in the basilar artery (16), which is consistent with our findings.

Our study found that in the subgroup of patients with DM, patients in the PR group were more likely to be female. This result suggests that sex differences may exist in PR. This may be related to the estrogen levels. Studies have found that estrogen affects the vascular system to induce vasodilation, increasing the bioavailability of nitric oxide (NO). It also modulates the renin-angiotensin aldosterone system (RAAS) and the sympathetic nervous system (38,39). These may all affect the vascular remodeling process, making female patients more likely to undergo PR. However, the exact mechanism of this sex difference is still unclear; multiple factors, including hormones, genetics, physiology, and behavior, are likely to be involved. Furthermore, factors such as sample size, study design and differences in study population may also have had an impact on the results. Future further studies and confirmation are needed.

Furthermore, the TG, FBG, and TyG index levels in the PR group were significantly higher than those in the non-PR group in the non-DM group, whereas no such difference was observed in the DM group. This is the first study that we are aware of to compare DM and non-DM patients with AIS, and to evaluate the correlation between the TyG index and vascular remodeling mode. When comparing DM and non-DM patients, it appears that the TyG index level may more accurately predict intracranial vessel PR. However, we found no difference in TyG index level between the two vascular remodeling modes in DM patients with AIS, despite the fact that IR is a key pathophysiological pathway for DM. Different metabolic imbalances and vascular effects may explain the complex mechanism of DM leading to differences in vascular remodeling modes (40). Different states, such as hyperglycemia, elevated free fatty acids, IR (41,42), and decreased vessel wall shearing stress (43), are involved in the vascular remodeling of DM patients, which have long-term and chronic effects and may interact to cause different vascular effects. Therefore, compared to DM patients, IR may have a greater effect on PR in non-DM patients, and differences in the TyG index level between remodeling modes may be more significant. This may explain our findings. Future research is required to evaluate the significance of the TyG index level in predicting the intracranial vascular remodeling mode in AIS patients.

There are also some limitations to this study, which must be considered when interpreting the results. As this is a retrospective study, we can only demonstrate the association between the TyG index and the intracranial vascular remodeling mode, but not their causality. Second, considering the number of patients analyzed in this study is 123, the bias from this initial selection is not negligible, and may have substantially affected the findings. Third, the study, based on hospitalized patients with AIS from a single center in China, involves a relatively small sample size, requiring replication in a larger-scale cohort of individuals from other races. Lastly, the absence of a long-term follow-up study, which may influence the relationship between the TyG index and the intracranial vascular remodeling mode in patients, warrants additional research.

Conclusions

TyG index is significantly correlated with intracranial arterial PR in patients with AIS. TyG index level may be a useful marker for predicting intracranial vessel PR, particularly in non-DM patients.

Acknowledgments

We would like to acknowledge the hard and dedicated

work of all the staff that implemented the intervention and evaluation components of the study.
Funding: This study was supported by Hebei Medical Science Research Project (No. 20200048) and Medical Applicable Technology Tracking Project of Hebei Province (No. GZ2022013).

Footnote

Reporting Checklist: The authors have completed the STROBE reporting checklist. Available at https://qims.amegroups.com/article/view/10.21037/qims-23-752/rc

Conflicts of Interest: All authors have completed the ICMJE uniform disclosure form (available at https://qims.amegroups.com/article/view/10.21037/qims-23-752/coif). The authors have no conflicts of interest to declare.

Ethical Statement: The authors are accountable for all aspects of the work in ensuring that questions related to the accuracy or integrity of any part of the work are appropriately investigated and resolved. This study was conducted in accordance with the Declaration of Helsinki (as revised in 2013) and approved by the Ethics Committee of the Second Hospital of Hebei Medical University. Written informed consent was provided by all participants.

References

1. Katan M, Luft A. Global Burden of Stroke. Semin Neurol 2018;38:208-11.
2. Wang Y, Zhao X, Liu L, Soo YO, Pu Y, Pan Y, Wang Y, Zou X, Leung TW, Cai Y, Bai Q, Wu Y, Wang C, Pan X, Luo B, Wong KS; . Prevalence and outcomes of symptomatic intracranial large artery stenoses and occlusions in China: the Chinese Intracranial Atherosclerosis (CICAS) Study. Stroke 2014;45:663-9.
3. Fang YC, Yeh CH. Role of microRNAs in Vascular Remodeling. Curr Mol Med 2015;15:684-96.
4. Fukuda K, Iihara K, Maruyama D, Yamada N, Ishibashi-Ueda H. Relationship between carotid artery remodeling and plaque vulnerability with T1-weighted magnetic resonance imaging. J Stroke Cerebrovasc Dis 2014;23:1462-70.
5. Deng XL, Liu Z, Wang C, Li Y, Cai Z. Insulin resistance in ischemic stroke. Metab Brain Dis 2017;32:1323-34.
6. Jeong S, Lee JH. The verification of the reliability of a triglyceride-glucose index and its availability as an advanced tool. Metabolomics 2021;17:97.
7. Toro-Huamanchumo CJ, Urrunaga-Pastor D, Guarnizo-Poma M, Lazaro-Alcantara H, Paico-Palacios S, Pantoja-Torres B, Ranilla-Seguin VDC, Benites-Zapata VA; . Triglycerides and glucose index as an insulin resistance marker in a sample of healthy adults. Diabetes Metab Syndr 2019;13:272-7.
8. Yki-Järvinen H. Liver fat in the pathogenesis of insulin resistance and type 2 diabetes. Dig Dis 2010;28:203-9.
9. Tanase DM, Gosav EM, Costea CF, Ciocoiu M, Lacatusu CM, Maranduca MA, Ouatu A, Floria M. The Intricate Relationship between Type 2 Diabetes Mellitus (T2DM), Insulin Resistance (IR), and Nonalcoholic Fatty Liver Disease (NAFLD). J Diabetes Res 2020;2020:3920196.
10. Wu Z, Wang J, Li Z, Han Z, Miao X, Liu X, Li X, Wang W, Guo X, Tao L. Triglyceride glucose index and carotid atherosclerosis incidence in the Chinese population: A prospective cohort study. Nutr Metab Cardiovasc Dis 2021;31:2042-50.
11. Wang A, Tian X, Zuo Y, Zhang X, Wu S, Zhao X. Association between the triglyceride-glucose index and carotid plaque stability in nondiabetic adults. Nutr Metab Cardiovasc Dis 2021;31:2921-8.
12. Won KB, Park GM, Lee SE, Cho IJ, Kim HC, Lee BK, Chang HJ. Relationship of insulin resistance estimated by triglyceride glucose index to arterial stiffness. Lipids Health Dis 2018;17:268.
13. Won KB, Park EJ, Han D, Lee JH, Choi SY, Chun EJ, Park SH, Han HW, Sung J, Jung HO, Chang HJ. Triglyceride glucose index is an independent predictor for the progression of coronary artery calcification in the absence of heavy coronary artery calcification at baseline. Cardiovasc Diabetol 2020;19:34.
14. Zhang D, Wang M, Wu L, Zhao Y, Wang S, Yin X, Wu X. Assessing the characteristics and diagnostic value of plaques for patients with acute stroke using high-resolution magnetic resonance imaging. Quant Imaging Med Surg 2022;12:1529-38.

15. Yu YN, Liu MW, Villablanca JP, Li ML, Xu YY, Gao S, Feng F, Liebeskind DS, Scalzo F, Xu WH. Middle Cerebral Artery Plaque Hyperintensity on T2-Weighted Vessel Wall Imaging Is Associated with Ischemic Stroke. AJNR Am J Neuroradiol 2019;40:1886-92.
16. Lu SS, Xie J, Su CQ, Ge S, Shi HB, Hong XN. Plasma homocysteine levels and intracranial plaque characteristics: association and clinical relevance in ischemic stroke. BMC Neurol 2018;18:200.
17. Li S, Song X, Hu Q, Zhao J, Du H, Yan Y, Wang G, Chen X, Wang Q. Association of Plaque Features with Infarct Patterns in Patients with Acutely Symptomatic Middle Cerebral Artery Atherosclerotic Disease. J Stroke Cerebrovasc Dis 2021;30:105724.
18. Cao X, Yang Q, Tang Y, Pan L, Lai M, Yu Z, Geng D, Zhang J. Normalized wall index, intraplaque hemorrhage and ulceration of carotid plaques correlate with the severity of ischemic stroke. Atherosclerosis 2020;315:138-44.
19. Jiao S, Huang J, Chen Y, Song Y, Gong T, Lu J, Guo T, Zhang J, Zhang C, Chen M. Impacts of Glycemic Control on Intracranial Plaque in Patients with Type 2 Diabetes Mellitus: A Vessel Wall MRI Study. AJNR Am J Neuroradiol 2021;42:75-81.
20. Choi YJ, Jung SC, Lee DH. Vessel Wall Imaging of the Intracranial and Cervical Carotid Arteries. J Stroke 2015;17:238-55.
21. Han Y, Qiao H, Chen S, Jing J, Pan Y, Li D, Liu Y, Meng X, Wang Y, Zhao X; . Intracranial artery stenosis magnetic resonance imaging aetiology and progression study: Rationale and design. Brain Behav 2018;8:e01154.
22. Shi Z, Zhao M, Li J, Meddings Z, Shi Y, Jiang T, Liu Q, Deng B, Lu J, Teng Z. Association of Hypertension With Both Occurrence and Outcome of Symptomatic Patients With Mild Intracranial Atherosclerotic Stenosis: A Prospective Higher Resolution Magnetic Resonance Imaging Study. J Magn Reson Imaging 2021;54:76-88.
23. Sánchez-García A, Rodríguez-Gutiérrez R, Mancillas-Adame L, González-Nava V, Díaz González-Colmenero A, Solis RC, Álvarez-Villalobos NA, González-González JG. Diagnostic Accuracy of the Triglyceride and Glucose Index for Insulin Resistance: A Systematic Review. Int J Endocrinol 2020;2020:4678526.
24. Almeda-Valdés P, Bello-Chavolla OY, Caballeros-Barragán CR, Gómez-Velasco DV, Viveros-Ruiz T, Vargas-Vázquez A, Aguilar-Salinas CA. Índices para la evaluación de la resistencia a la insulina en individuos mexicanos sin diabetes. Gac Med Mex 2018;154:S50-5.
25. Guerrero-Romero F, Simental-Mendía LE, González-Ortiz M, Martínez-Abundis E, Ramos-Zavala MG, Hernández-González SO, Jacques-Camarena O, Rodríguez-Morán M. The product of triglycerides and glucose, a simple measure of insulin sensitivity. Comparison with the euglycemic-hyperinsulinemic clamp. J Clin Endocrinol Metab 2010;95:3347-51.
26. Kim SH, Moon JY, Lim YM, Kim KH, Yang WI, Sung JH, Yoo SM, Kim IJ, Lim SW, Cha DH, Cho SY. Association of insulin resistance and coronary artery remodeling: an intravascular ultrasound study. Cardiovasc Diabetol 2015;14:74.
27. Qiao Y, Anwar Z, Intrapiromkul J, Liu L, Zeiler SR, Leigh R, Zhang Y, Guallar E, Wasserman BA. Patterns and Implications of Intracranial Arterial Remodeling in Stroke Patients. Stroke 2016;47:434-40.
28. Kanazawa M, Ninomiya I, Hatakeyama M, Takahashi T, Shimohata T. Microglia and Monocytes/Macrophages Polarization Reveal Novel Therapeutic Mechanism against Stroke. Int J Mol Sci 2017;18:2135.
29. Wang X, Khalil RA. Matrix Metalloproteinases, Vascular Remodeling, and Vascular Disease. Adv Pharmacol 2018;81:241-330.
30. Mishani S, Belhoul-Fakir H, Lagat C, Jansen S, Evans B, Lawrence-Brown M. Stress distribution in the walls of major arteries: implications for atherogenesis. Quant Imaging Med Surg 2021;11:3494-505.
31. Xu H, Li X, Adams H, Kubena K, Guo S. Etiology of Metabolic Syndrome and Dietary Intervention. Int J Mol Sci 2018;20:128.
32. Zhang F, Zhang Y, Guo Z, Yang H, Ren M, Xing X, Cong H. The association of triglyceride and glucose index, and triglyceride to high-density lipoprotein cholesterol ratio with prehypertension and hypertension in normoglycemic subjects: A large cross-sectional population study. J Clin Hypertens (Greenwich) 2021;23:1405-12.
33. Humphrey JD. Mechanisms of Vascular Remodeling in Hypertension. Am J Hypertens 2021;34:432-41.
34. Peng J, Luo F, Ruan G, Peng R, Li X. Hypertriglyceridemia and atherosclerosis. Lipids Health Dis 2017;16:233.
35. Talayero BG, Sacks FM. The role of triglycerides in atherosclerosis. Curr Cardiol Rep 2011;13:544-52.
36. Wang S, Li Z, Li X, Gao Q, Liu X, Wei Q, Guo C, Zhao X, Chen L. Plasma ApoB/AI: An effective indicator for intracranial vascular positive remodeling. J Neurol Sci 2022;436:120226.
37. Chen L, Lei L, Li T, Yan J, Jiang J. A20 alleviates the vascular remodeling induced by homocysteine. Am J

Transl Res 2018;10:3991-4003.
38. Di Giosia P, Giorgini P, Stamerra CA, Petrarca M, Ferri C, Sahebkar A. Gender Differences in Epidemiology, Pathophysiology, and Treatment of Hypertension. Curr Atheroscler Rep 2018;20:13.
39. Chaudhari S, Cushen SC, Osikoya O, Jaini PA, Posey R, Mathis KW, Goulopoulou S. Mechanisms of Sex Disparities in Cardiovascular Function and Remodeling. Compr Physiol 2018;9:375-411.
40. Yahagi K, Kolodgie FD, Lutter C, Mori H, Romero ME, Finn AV, Virmani R. Pathology of Human Coronary and Carotid Artery Atherosclerosis and Vascular Calcification in Diabetes Mellitus. Arterioscler Thromb Vasc Biol 2017;37:191-204.
41. Virmani R, Burke AP, Kolodgie F. Morphological characteristics of coronary atherosclerosis in diabetes mellitus. Can J Cardiol 2006;22 Suppl B:81B-4B.
42. Creager MA, Lüscher TF, Cosentino F, Beckman JA. Diabetes and vascular disease: pathophysiology, clinical consequences, and medical therapy: Part I. Circulation 2003;108:1527-32.
43. Chytilová E, Malík J, Kasalová Z, Doležalová R, Stulc T, Ceska R. Lower wall shear rate of the common carotid artery in treated type 2 diabetes mellitus with metabolic syndrome. Physiol Res 2009;58:185-91.

Cite this article as: Niu YN, Guo C, Guo XZ, Wei Q, Zhou X, Li M, Xia JN, Chen LP. High-resolution magnetic resonance imaging investigation of the connection between the triglyceride-glucose index and intracranial arterial remodeling: a retrospective cross-sectional study. Quant Imaging Med Surg 2023;13(12):8504-8516. doi: 10.21037/qims-23-752

